



Published in final edited form as:

Cell Host Microbe. 2012 January 19; 11(1): 46–57. doi:10.1016/j.chom.2011.11.009.

The *Legionella pneumophila* effector DrrA is sufficient to stimulate SNARE-dependent membrane fusion

Kohei Arasaki^{1,2}, Derek K. Toomre³, and Craig R. Roy^{1,*}

¹Section of Microbial Pathogenesis, Yale University School of Medicine, New Haven, CT 06526

²School of Life Sciences, Tokyo University of Pharmacy and Life Sciences Horinouchi, Hachioji, Tokyo 192-0392, Japan

³Department of Cell Biology, Yale University School of Medicine, New Haven, CT 06535

Summary

The intracellular bacterial pathogen *Legionella pneumophila* subverts host membrane transport pathways to promote fusion of vesicles exiting the endoplasmic reticulum (ER) with the pathogen-containing vacuole. During infection there is non-canonical pairing of the SNARE protein Sec22b on ER-derived vesicles with plasma membrane (PM)-localized syntaxin proteins on the vacuole. We show that the *L. pneumophila* Rab1-targeting effector DrrA is sufficient to stimulate this non-canonical SNARE association and promote membrane fusion. DrrA activation of the Rab1 GTPase on PM-derived organelles stimulated the tethering of ER-derived vesicles with the PM-derived organelle resulting in vesicle fusion through the pairing of Sec22b with the PM syntaxin proteins. Thus, the effector protein DrrA stimulates a host membrane transport pathway that enables ER-derived vesicles to remodel a PM-derived organelle, suggesting that Rab1 activation at the PM is sufficient to promote the recruitment and fusion of ER-derived vesicles.

Keywords

Legionella pneumophila; Dot/Icm; DrrA/SidM; SNARE; membrane fusion; syntaxin; Sec22b; plasma membrane and ER-derived vesicle

Introduction

Legionella pneumophila is a gram-negative bacterium that has the ability to replicate in phagocytes by creating a vacuole that avoids endocytic maturation (Horwitz, 1983). ER-derived vesicles are rapidly recruited and remodel the PM-derived organelle harboring *Legionella* by a process mediated by the type IV secretion system called Dot/Icm (Berger and Isberg, 1993; Roy et al., 1998; Segal et al., 1998; Swanson and Isberg, 1995; Tilney et al., 2001; Vogel et al., 1998) }.

The Dot/Icm apparatus delivers bacterial proteins known as effectors into the host cell (Nagai et al., 2002). The *Legionella* genome encodes over 200 proteins translocated into host cells by the Dot/Icm system (Ensminger and Isberg, 2009). Although the biochemical

© 2011 Elsevier Inc. All rights reserved.

*Correspondence: craig.roy@yale.edu.

Publisher's Disclaimer: This is a PDF file of an unedited manuscript that has been accepted for publication. As a service to our customers we are providing this early version of the manuscript. The manuscript will undergo copyediting, typesetting, and review of the resulting proof before it is published in its final citable form. Please note that during the production process errors may be discovered which could affect the content, and all legal disclaimers that apply to the journal pertain.

activities of most effectors remain to be determined, the few effectors that have been studied in detail include proteins that modulate the function of GTPases that regulate host membrane transport. These include the protein RalF, which is an Arf guanine nucleotide exchange factor (GEF) (Nagai et al., 2002), and several proteins that modulate Rab1 function (Ingmundson et al., 2007; Machner and Isberg, 2006, 2007; Murata et al., 2006).

The DrrA protein (also called SidM) is a well-characterized effector targeting Rab1 (Ingmundson et al., 2007; Machner and Isberg, 2006, 2007; Murata et al., 2006). Three functional domains in DrrA (Figure 1A) have been defined biochemically and resolved structurally (Muller et al., 2010; Schoebel et al., 2009; Suh et al., 2009; Zhu et al., 2010). The carboxyl-terminal region of DrrA contains a phosphatidylinositol 4-phosphate (PI4P) binding domain (Brombacher et al., 2009; Schoebel et al., 2010; Zhu et al., 2010) that targets DrrA to the host PM (Murata et al., 2006). The central region of DrrA contains a Rab1-specific GEF domain that can displace Rab-GDI bound to inactive Rab1 (Schoebel et al., 2009; Suh et al., 2009; Zhu et al., 2010). The amino-terminal region of DrrA has an adenylyltransferase (ATase) domain that uses ATP as a substrate to attach an AMP residue to a conserved tyrosine residue in the switch 2 region of activated Rab1-GTP, making Rab1 insensitive to GTPase-activating proteins (GAPs) (Muller et al., 2010). Thus, DrrA mediates the recruitment and activation of Rab1 on the PM-derived vacuole that harbors *Legionella*.

Although mutations that eliminate the DrrA protein reduce the amount of Rab1 recruited to the LCV, the ability of *Legionella* to traffic correctly and remodel the *Legionella*-containing vacuole (LCV) is not compromised to a measurable degree in a *drrA* mutant, presumably because of the functional redundancy inherent in such a large repertoire of bacterial effectors (Ingmundson et al., 2007; Machner and Isberg, 2007). Functional redundancy has made it difficult to assess the contribution of individual effectors in LCV transport using standard genetic techniques. Thus, it is unclear why *Legionella* has acquired DrrA.

The molecular details of how ER-derived vesicles fuse with the LCV remain unknown, but host proteins involved in the transport of early secretory vesicles are involved. In addition to a possible role for Rab1 (Derre and Isberg, 2004; Kagan et al., 2004), membrane fusion between the LCV and ER-derived vesicles involves interactions between the v-SNARE Sec22b on the ER-derived vesicles and a PM t-SNARE complex containing host syntaxins (Arasaki and Roy, 2010). Here, we show that the DrrA protein promotes the tethering of ER-derived vesicles with the PM-derived organelle, which leads to membrane fusion through Sec22b interactions with PM-localized syntaxins.

Results

DrrA interacts with PM syntaxins

When coexpressed in mammalian cells the GFP-tagged DrrA₆₁₋₆₄₇ protein (Figure 1A) was detected in a coprecipitate with 3x-FLAG-tagged PM syntaxins (Stx2, Stx3, and Stx4) at higher levels compared to SNAREs SNAP23, Sec22b or the Golgi-localized syntaxin 3x-FLAG-Stx5 (Figure 1B). The DrrA₆₁₋₆₄₇ protein was used because it does not display host toxicity associated with the ATase domain but retains GEF and PI4P-binding activities (Figure 1A). The C-terminal region of DrrA containing a PI4P-binding domain that mediates PM localization was sufficient for the syntaxin interaction, as GFP-DrrA₄₅₁₋₆₄₇ coprecipitated more efficiently with the PM syntaxins compared to the control SNARE proteins SNAP23 or Sec22b (Figure 1C). GFP-tagged DrrA₄₅₁₋₆₄₇ coprecipitated with cytosolic derivatives of Stx2, Stx3 and Stx4 lacking their transmembrane domain (Figure 1D). By contrast, GFP-DrrA₆₁₋₆₄₇ protein did not efficiently interact with the cytosolic derivatives of these syntaxins (Figure 1D), suggesting an interaction between the DrrA₆₁₋₆₄₇ protein and these syntaxins requires additional factors at the membrane surface.

After infection of host cells by wild-type *Legionella*, endogenous DrrA was detected in association with 3x-FLAG-Stx3, whereas, DrrA was not detected in association with 3x-FLAG-Stx3 in cells infected with a *dotA* mutant strain that is unable to translocate DrrA into cells or in cells infected with the $\Delta drrA$ mutant (Figure 2A). Consistent with results using GFP-DrrA₆₁₋₆₄₇ expressed ectopically (Figure 1A), endogenous DrrA translocated during infection showed the highest affinity for 3x-FLAG-Stx3 followed by Stx4 (Figure 2B). An interaction between 3x-FLAG-Stx2 and translocated DrrA was below the threshold of detection in this assay (Figure 2B), consistent with DrrA binding to Stx2 being less efficient than Stx3 and Stx4 binding. Additionally, translocated DrrA was not detected in association with control proteins SNARE proteins SNAP23 or VAMP7. Thus, after translocation into host cells by *Legionella* the DrrA proteins associates with a complex containing PM syntaxins.

Rab1 facilitates binding of DrrA to Stx3

The ectodomain of syntaxin proteins contains a regulatory Habc region that binds the SNARE motif through an intramolecular interaction and chaperone proteins such as Munc18 bind to the Habc region to regulate SNARE interactions (Dietrich et al., 2003). To define regions required for interaction and understand the mechanisms that regulate these interactions, binding of DrrA to deletion derivatives of PM syntaxin proteins were examined by coprecipitation. These *in vivo* data revealed that the SNARE motif in the PM syntaxins was required for formation of a complex containing the GFP-DrrA₄₅₁₋₆₄₇ protein (Figure S1). To determine if DrrA interacts directly with the SNARE motif, MBP-tagged derivatives of Stx3 and His-tagged derivatives of DrrA were purified and tested for interaction *in vitro*. A direct interaction was observed between DrrA₄₅₁₋₆₄₇ and Stx3 derivatives containing the SNARE motif (Figure 3A, MBP-Stx3 $\Delta_{\text{Habc/TMD}}$ and MBP-Stx3 $\Delta_{\text{Habc/TMD}}$). DrrA₁₋₅₀₀ did not interact with the Stx3 proteins, indicating that the C-terminal domain of DrrA is both sufficient and necessary for binding. The intact Habc region in Stx3 prevented this *in vitro* interaction (Figure 3A, MBP-Stx3 Δ_{TMD}), similar to what was observed with the positive control protein SNAP23, which is a cognate SNARE that interacts with Stx3 through SNARE motif interactions. This suggests that the Habc region and DrrA₄₅₁₋₆₄₇ have overlapping binding sites in the SNARE motif, and that chaperone proteins inside the cell that bind to the Habc domain can expose the SNARE motif for DrrA recognition *in vivo*, enabling DrrA to interact with the full-length Stx3 protein in cells. The interaction between DrrA₄₅₁₋₆₄₇ and MBP-Stx5 $\Delta_{\text{Habc/TMD}}$ and MBP-Stx5 $\Delta_{\text{Habc/TMD}}$ was lower compared to the analogous Stx3 interactions, indicating that DrrA binds preferentially to the SNARE motif of Stx3 (Figure 3B).

When compared to DrrA₄₅₁₋₆₄₇, the full-length DrrA₁₋₆₄₇ protein was less efficient at forming a complex with the SNARE motif of Stx3 under these *in vitro* conditions (Figure 3A). One explanation is that the central region of DrrA in the context of the full-length protein regulates the ability of the C-terminal region to interact with syntaxins by conferring an auto-inhibitory function that would be relieved *in vivo* during Rab1 binding, which is consistent with the *in vivo* data (Figure 1D). This suggests that an interaction between the DrrA₆₁₋₆₄₇ protein and these syntaxins could be regulated by factors at the membrane surface. Consistent with this hypothesis, incubation of full-length DrrA with the GDP-locked variant of Rab1 (GST-Rab1_{S25N}), which was shown previously to bind tightly to DrrA (Ingmundson et al., 2007; Machner and Isberg, 2006, 2007; Murata et al., 2006), enhanced complex formation between DrrA and Stx3 (Figure 3C). By contrast, the addition of the GTP-locked variant Rab1_{Q70L}, which does not bind DrrA tightly, did not enhance Stx3 complex formation (Figure 3C). Similarly, when wild type Rab1 was added to DrrA in the absence of GTP to prevent nucleotide exchange, enhanced complex formation between full-length DrrA and Stx3 was observed in manner that was dependent on the amount of

Rab1 in the reaction (Figure 3C-E). By contrast, the binding of DrrA to Stx3 *in vitro* was reduced under condition where the stable association of Rab1 and full-length DrrA was abrogated by the inclusion of GTP (Figure 3C,D).

Because the ATase domain of DrrA can use GTP as a substrate to GMPylate Rab1 (Muller et al., 2010), the full length DrrA protein was compared in this assay to the DrrA₃₄₀₋₆₄₇ protein, which has the ATase domain deleted but retains an intact GEF and PI4P binding domain. The full-length DrrA protein and the DrrA₃₄₀₋₆₄₇ protein gave similar results in this assay (Figure 3D, compare DrrA₁₋₆₄₇ to DrrA₃₄₀₋₆₄₇), which demonstrates that the inactive Rab1 protein enhanced binding of full-length DrrA to Stx3 observed in this *in vitro* assay was dependent on stable interactions between Rab1 and the GEF domain of DrrA and not on Rab1 GMPylation mediated by the ATase domain. These results suggest that a region near the carboxyl terminus of DrrA interacts with Stx3, and Rab1 binding to the full-length DrrA protein facilitates this interaction.

DrrA promotes non-canonical SNARE pairing

DrrA and Stx3 association was coordinated by Rab1 activation, further supporting that DrrA might promote Rab1-dependent membrane tethering and fusion events. Given data indicating that *Legionella* infection promotes a functional interaction between Stx3 and Sec22b, we asked whether DrrA was sufficient to promote this non-canonical SNARE interaction. Vesicles derived from the ER were isolated in a post nuclear supernatant (PNS) fraction from HEK293-FcγRII cells that stably express 3x-FLAG-Sec22b. Amylose beads containing MBP-Stx3, DrrA, and Rab1 or MBP-Stx3 and DrrA₄₅₁₋₆₄₇ were incubated with the PNS fraction with or without GDP or GTP. The pairing of Sec22b on the vesicles with purified MBP-Stx3 in the reaction was measured by coprecipitation of proteins associated with MBP-Stx3 on the amylose beads. These data demonstrate that in the reaction containing full-length DrrA and GTP, the binding of MBP-Stx3 to the 3x-FLAG-Sec22b associated with the vesicles was enhanced more than five fold (Figure 4, 3x-FLAG-Sec22b lane), indicating that Rab1 activation by DrrA stimulated the association of Stx3 and Sec22b.

A digitonin permeabilization system (Traub et al., 1996) that allows the diffusion of untethered vesicles across the PM of semi-intact cells (Aoki et al., 2009; Jesch and Linstedt, 1998; Zolov and Lupashin, 2005) was used to further investigate DrrA-mediated assembly of a Sec22b and Stx3 SNARE complex. Cells producing both GFP-Stx3 and derivatives of GFP-DrrA were permeabilized partially with digitonin and incubated with a PNS fraction containing ER-derived vesicles from cells producing 3x-FLAG-Sec22b. The binding of vesicle-associated Sec22b to PM-localized GFP-Stx3 was analyzed by coprecipitation. A GTP-dependent interaction between GFP-Stx3 and 3x-FLAG-Sec22b was detected in cells producing derivatives of DrrA with an intact GEF domain and PI4P-binding domain (Figure 5A, GFP-DrrA₆₁₋₆₄₇ and GFP-DrrA₂₀₁₋₆₄₇). By contrast, GFP-DrrA₄₅₁₋₆₄₇, which does not have an intact GEF domain but retains the PI4P-binding domain and has the ability to interact with Stx3, did not promote an interaction between Stx3 and Sec22b, supporting that Rab1 activation by DrrA is important for stimulating formation of this SNARE complex (Figure 5A). Because functional SNARE pairs are recognized and dissociated by a complex consisting of α SNAP and NSF, purified NSF and α -SNAP were added to the reactions before the immunoprecipitation of 3x-FLAG-Sec22b to determine whether these factors dissociated Stx3 from the complex. The addition of NSF and α -SNAP resulted in a reduction in the association of Stx3 and Sec22b, indicating that the complex formed upon the addition of DrrA represents a functional SNARE assembly (Figure 5B). Thus, the ability of DrrA to recruit and activate Rab1 at the PM can initiate the assembly of a SNARE complex containing Stx3 and Sec22b.

DrrA activation of Rab1 promotes the tethering ER-derived vesicles with PM-derived organelles

Rab proteins play an important role in promoting the tethering of vesicles to target membranes, and this will promote membrane fusion if compatible SNARE proteins are present on juxtaposed membranes. Our data suggest that ER-derived vesicles are recruited to PM-derived organelles following DrrA-mediated activation of Rab1, and that tethering of these vesicles promotes this non-canonical SNARE interaction. To investigate this further, cells permeabilized with digitonin were incubated with PNS from cells producing a YFP-KDEL protein localized to the lumen of ER-derived vesicles (Figure S2A). Fluorescence microscopy showed that DrrA stimulated the tethering of ER-derived vesicles containing YFP-KDEL with the permeabilized cells (Figure S2B). This tethering of the ER-derived vesicles required the GEF domain in DrrA and the addition of GTP, suggesting that Rab1 activation is important for the tethering reaction (Figure S2B). Silencing of host PM syntaxins by siRNA in the permeabilized acceptor cells did not affect DrrA-mediated tethering of the ER-derived vesicles (Figure S2C), consistent with vesicle tethering being independent of SNARE interactions. Upon addition of a “fusion buffer” consisting of a fresh cytosolic protein extract and abundant levels of ATP, there was a loss in the YFP-KDEL fluorescence that required the expression of PM syntaxins in the acceptor cells (Figure S2C). These data are consistent with SNARE-mediated fusion with the PM resulting in release of the YFP-KDEL from the lumen of the ER-derived vesicles.

Tethering of ER-derived vesicles at the PM was also visualized using total internal reflection fluorescence (TIRF) microscopy. Single ER-derived vesicles labeled with RFP-KDEL were observed tethered in an induced evanescent field at the PM of permeabilized cells by a process requiring DrrA and GTP (Figure 6 and S2D). Upon the addition of fusion buffer, most vesicles lost fluorescence over a reaction period of 30 sec, suggesting fusion of the vesicles with the PM resulted in release of the luminal RFP-KDEL probe from the tethered vesicles into the extracellular environment. Silencing of the PM syntaxins in the acceptor cells, or silencing of Sec22b on ER-derived vesicles obtained from the donor cells, did not affect the tethering reaction (Figure 6 and S2E), but did interfere with the loss in fluorescence observed upon the addition of fusion buffer (Figure 6). Thus, Rab1 activation by DrrA promotes the tethering of ER-derived vesicles to a PM-derived organelle, and Sec22b interactions with the PM syntaxins potentially promote vesicle fusion.

DrrA activates a host pathway that promotes the fusion of ER-derived vesicles with a PM-derived organelle

To corroborate that the loss in fluorescence observed by TIRF microscopy was a valid indicator of membrane fusion, donor vesicles with soluble Luciferase-KDEL restricted to the lumen were employed in the permeabilized cell assay. Fusion of the ER-derived vesicles with the PM should release the soluble Luciferase-KDEL protein contained in the lumen of the tethered vesicles. Thus, fusion will result in an increase in the ratio of Luciferase-KDEL in the soluble extracellular fraction compared to the membrane pellet. Similar to the imaging data, DrrA stimulated donor vesicles containing Luciferase-KDEL to associate with acceptor membranes by a process requiring GTP, as indicated by the increase in Luciferase activity associated with permeabilized cells following the tethering reaction (Figure 7A). A requirement for Rab1 in the tethering reaction was indicated by a reduction in vesicle association upon the addition of GDP-locked Rab1 to the reaction, and by using PNS obtained from cells in which Rab1 had been silenced by siRNA (Figure S3A-D). Silencing of host PM syntaxins or Sec22b did not reduce DrrA-mediated tethering of ER-derived vesicles with the permeabilized cells (Figure 7B). The addition of fusion buffer stimulated release of Luciferase from the lumen of tethered ER-derived vesicles into the supernatant fraction of the reaction (Figure 7B). Luciferase release was blocked by NEM (Figure S3E),

which prevents SNARE-mediated fusion reactions by interfering with the disassembly of cis-SNARE complexes by NSF and α -SNAP. These data are consistent with the release of Luciferase from the ER-derived vesicles being the result of PM fusion.

If the Luciferase release represents a *bona fide* SNARE-mediated membrane fusion event, it should require specific SNARE proteins oriented correctly on the vesicles and target membranes. Indeed, silencing of Sec22b on donor vesicles containing Luciferase-KDEL interfered with fusion, whereas, silencing of the PM syntaxins in the donor cells had no effect on fusion (Figure 7B). By contrast, silencing of the ER-localized syntaxin proteins Stx17 or Stx18 in the donor cells did not affect fusion (Figure S3F), indicating a specific role for Sec22b on the ER-derived vesicles in the fusion reaction. Similarly, silencing of PM syntaxins in the acceptor cells interfered with fusion of the ER-derived vesicles, but silencing of Sec22b in the acceptor cells had no significant impact on membrane fusion (Figure 7B). Thus, the fusion process was specific for Sec22b being the v-SNARE on the ER-derived vesicles and PM syntaxins functioning as a t-SNARE.

To independently validate that DrrA was directing the tethering and fusion of ER-derived vesicles with the PM, a GFP-tagged derivative of a temperature-sensitive vesicular stomatitis virus glycoprotein (ts045-VSVG) was used in the permeabilized cell assay to determine whether this transmembrane protein could be delivered from ER-derived vesicles to the PM. Fluorescent vesicles were obtained at different times after cells were shifted to a temperature that permits ts045-VSVG-GFP to exit the ER. The ts045-VSVG-GFP protein was localized primarily to pre-Golgi compartments 15 minutes after incubating cells at the permissive temperature (Figure S3G), and vesicles generated from these cells could be tethered to semi-intact cells in the presence of DrrA (Figure S3H). By contrast, ts045-VSVG-GFP was localized primarily to post-Golgi compartments 90 minutes after incubating cells at the permissive temperature and fluorescent vesicles generated from these cells were not tethered to semi-intact cells incubated with DrrA (Figure S3H). This indicates that DrrA preferentially directs the tethering of ER-derived vesicles to target membranes. TIRF microscopy validated that the vesicles containing ts045-VSVG-GFP were associated with the PM and that tethering was not affected by the silencing of PM syntaxins (Figure 7C, before fusion). After addition of fusion buffer (Figure 7C, after fusion), there was a redistribution of ts045-VSVG-GFP from the tethered vesicles to the PM of the recipient cells (no siRNA), which is consistent with fusion of the ER-derived vesicles. By contrast, ts045-VSVG-GFP remained localized to the tethered vesicles when PM syntaxins were silenced in the recipient cells (Stx2/3/4 KD). Thus, DrrA-mediated activation of Rab1 at the PM is sufficient to recruit ER-derived vesicles and promote their fusion through the non-canonical pairing of Sec22b and PM syntaxins (Figure 7D).

Discussion

A working model summarizes our principle findings of how DrrA directs the fusion of ER-derived vesicles with the PM-derived organelle containing *Legionella* and underscores new open questions (Figure 7D). Stage 1 depicts interactions mediated by the GEF domain and the PI4P-binding domain of DrrA. Our data indicate that the DrrA carboxy-terminal region interacts directly with PM-localized syntaxins (Figure 1), providing an additional function to a domain that was previously shown to have a PI4P binding activity important for localization of DrrA to PM-derived organelles (Brombacher et al., 2009; Schoebel et al., 2010; Zhu et al., 2010). The interaction with Stx3 and the full-length DrrA protein was observed upon infection of *Legionella* (Figure 2), and could be enhanced *in vitro* by the binding of inactive GDP-bound Rab1 to the GEF domain (Figure 3). The dynamics of Rab1 activation by the GEF domain in DrrA leads to the accumulation of Rab1-GTP on the PM-derived compartment and interactions mediated by the PI4P-binding domain in DrrA would

facilitate the localization of syntaxins to this region of the membrane. Thus, these activities of DrrA serve to localize host factors that participate in the tethering and fusion of ER-derived vesicles with the PM-derived organelle.

Stage 2 depicts the Rab1-dependent tethering of ER-derived vesicles to the PM-derived compartment. This stage is supported by data showing in permeabilized cells that the tethering of ER-derived vesicles to the PM required DrrA with a functional GEF domain, Rab1, and GTP (Figures S3-S5 and Figure 7A). A role for SNARE proteins in the tethering stage was not apparent, as silencing of either Sec22b or PM syntaxins did not reduce vesicle tethering stimulated by DrrA. Given that Rab-mediated vesicle tethering in cells usually involves a protein that binds to a GTP-bound Rab protein on the acceptor membrane and associates with factors on the membrane of the donor vesicle, an unidentified tethering factor that binds to active Rab1 and interacts with the ER-derived vesicle is depicted in this model. This protein could be a factor that normally associates with early secretory vesicles and binds active Rab1 on Golgi or pre-Golgi membranes. Alternatively, this tethering factor could be a protein that is not typically associated with early secretory vesicles. Future studies are needed to determine the identity of this putative tethering factor and other host factors that may participate in this Rab1-mediated tethering reaction.

Stage 3 depicts the functional association of Sec22b on the ER-derived vesicles with the PM Stx3 protein. Our data indicate that formation of this complex can be stimulated by DrrA-mediated activation of Rab1 (Figure 4). Interestingly, homologues of these SNARE proteins from *Saccharomyces cerevisiae* promote membrane fusion *in vitro* when incorporated into synthetic vesicles, however, it was argued that fusion of ER-derived vesicles with the PM would be restricted topologically by cellular mechanisms that regulate vesicle tethering *in vivo* (McNew et al., 2000). Consistent with this hypothesis, our model predicts that the tethering reaction mediated by activated Rab1 at the PM is sufficient to overcome this topological restriction and promote functional interactions between Sec22b and PM syntaxins. Thus, the primary role of DrrA in promoting the tethering of ER-derived vesicles with the PM is to overcome this topological restriction by activating Rab1 on this organelle.

Stage 4 depicts the fusion of ER-derived vesicles with the PM-derived organelle. Independent indicators of this fusion reaction are provided by data showing the DrrA-mediated release of the soluble Luciferase-KDEL protein contained in the lumen of ER-derived vesicles and the delivery of the transmembrane protein ts045-VSVG-GFP from the limiting membrane of ER-derived vesicles to the surface of cells (Figure 7). Fusion of ER-derived vesicles with the PM resulting from DrrA-mediated activation of Rab1 was blocked when PM syntaxins were reduced on the acceptor compartment or when Sec22b was reduced on the donor compartments, demonstrating fusion involves a topological requirement for these SNAREs on distinct organelles. SNAP23 is depicted as also being involved in this fusion process based on data showing fusion of synthetic liposomes with a t-SNARE complex consisting of the SNAP23 homologue Sec9p and the PM syntaxin homologue Sso1p with liposomes that display the v-SNARE Sec22p (McNew et al., 2000).

Importantly, the observation that DrrA was sufficient to promote the tethering and fusion of ER-derived vesicles with the PM indicates that no additional bacterial factors are required to promote this reaction. In the context of *Legionella* infection, however, other effector proteins are predicted to enhance the efficiency of this pathway. Notably, the *Legionella* effector LidA binds to Rab1, and immobilization of LidA and DrrA to paramagnetic beads is sufficient to stimulate the tethering of ER-derived vesicles to beads by a Rab1-dependent mechanism (Machner and Isberg, 2006, 2007). Thus, LidA should enhance DrrA-mediated fusion of ER-derived vesicles with the PM-derived organelle. Additionally, the observation that Dot/Icm-dependent Sec22b and Stx3 interactions are detected during infection of host

cells by a $\Delta drrA$ mutant (Arasaki and Roy, 2010) indicate that there should be *Legionella* effectors that promote tethering of ER-derived vesicles to the LCV membrane by a process that does not require DrrA function. Possibilities include effectors that mimic active Rab1 or mimic the tethering factors Rab1 recruits to the LCV. Tethering mediated by these effectors would then promote the engagement of PM syntaxins and Sec22b, which would promote fusion of ER-derived vesicles with the LCV by a pathway that is independent of DrrA.

Lastly, these data may provide insight into cellular process that could direct the fusion of ER-derived vesicles with phagosome membranes during endocytic maturation. There are several independent studies that suggest the existence of an endogenous cellular pathway in phagocytic cells, such as macrophages, that enables ER-derived vesicles to fuse with phagosomes (Becker et al., 2005; Gagnon et al., 2002; Hatsuzawa et al., 2006). Immunological studies have indicated that fusion of ER with phagosomes is important for the delivery components that allow antigens in the lumen of phagosomes to be transported across a vacuole membrane and presented on MHC class I molecules (Ackerman et al., 2006; Guermontprez et al., 2003; Houde et al., 2003). However, it is difficult to detect fusion of ER-derived membranes with phagosomes by fluorescence microscopy (Touret et al., 2005) or by quantitative mass spectrometry (Rogers and Foster, 2007), suggesting if fusion of ER-derived membranes with phagosomes represents an endogenous transport pathway in cells, this process must be tightly regulated. Our data suggest that activation of Rab1 on the phagosome membrane would be sufficient to promote the recruitment of ER-derived vesicles, and fusion of these vesicles with the phagosomes would occur upon formation of the SNARE complex containing Sec22b and PM syntaxins. Thus, it will be interesting to know whether phagocytic cells produce a GEF that functions analogously to DrrA to regulate the recruitment and fusion of ER-derived vesicles with phagosomes, and if Sec22b and PM syntaxins are involved.

Experimental Procedures

Cell culture, siRNA, transfection, bacterial strain and infection

Maintenance of HEK293-Fc γ R2 cells and HEK293-Fc γ R2 3x-FLAG-Sec22b cells were described previously (Arasaki and Roy, 2010). RNA duplexes targeting Stx2, Stx3, Stx4, Stx17, Stx18, Sec22b, Rab1A and Rab1B purchased from Dharmacon as siRNAplusSmart Pools. Transfection of plasmid DNA or siRNA was performed using LipofectAmine 2000 (Invitrogen) according to the manufacturer's recommendation. Growth of *L. pneumophila* strains Lp01, the *dotA* mutant strain CR58 and the $\Delta drrA$ mutant were described previously (Coers et al., 2000; Murata et al., 2006; Nagai et al., 2002; Zuckman et al., 1999).

Antibodies

Rabbit polyclonal antibodies to GFP and SNAP23 were purchased from Invitrogen and Abcam, respectively. Mouse monoclonal antibodies to FLAG and His were obtained from Sigma Aldrich. Goat polyclonal antibody to GST and rabbit polyclonal antibody to MBP were purchased from GE healthcare and New England Biolabs, respectively. Rabbit polyclonal antibodies to Rab1A and Rab1B were purchased from Santa Cruz. Rabbit polyclonal antibodies to *Legionella* and DrrA were described (Murata et al., 2006).

Protein purification

Affinity purification of tagged proteins was conducted as described (Arasaki and Roy, 2010; Ingmundson et al., 2007; Murata et al., 2006). Proteins were dialyzed in buffer containing 100mM NaCl, 1mM MgCl₂ and 20mM Hepes-KOH (pH7.2).

Infection, immunoprecipitation and *in vitro* binding assay

Infection of HEK293-Fc γ RII cells with *Legionella* and generation of cell lysates for immunoprecipitation studies were conducted as described (Arasaki and Roy, 2010). For immunoprecipitation studies, lysates were incubated with anti-FLAG M2 beads for 1 hour at 4°C. After incubation, beads were washed extensively and 3x-FLAG fusion proteins were eluted using a 3x-FLAG peptide (final concentration; 100 μ g/ml). For *in vitro* binding assays, MBP fusion proteins were incubated with 10 μ l of amylose resin in binding buffer (100mM NaCl, 1mM MgCl₂, 20mM Hepes-KOH (pH7.2) containing 0.2% Triton X-100) for 3 hr at 4°C. The beads were washed extensively using binding buffer to remove unbound MBP fusion proteins and then mixed with His or GST fusion proteins in binding buffer overnight. Beads were washed extensively and resuspended in SDS-PAGE sample buffer for analysis.

Preparation of permeabilized cells and PNS fractions

HEK293-Fc γ RII cells were grown on poly-L-lysine (MW 75,000-150,000; Sigma Aldrich) coated tissue culture plates or 35mm glass bottom dishes. Cells were washed with permeabilization buffer (125mM KOAc, 2.5mM Mg(OAc)₂, 25mM Hepes-KOH (pH7.2), 1mg/ml glucose and 1mM DTT) and treated with 30 μ g/ml digitonin in permeabilization buffer for 5 min at room temperature. After treatment, permeabilized cells were washed with permeabilization buffer. To prepare PNS fractions, cells were resuspended in homogenization buffer (125mM KOAc, 2.5mM Mg(OAc)₂, 25mM Hepes-KOH (pH7.2), 0.25mM Sucrose, 1mM DTT and protease inhibitors) and disrupted using a ball bearing homogenizer. Homogenized cells were centrifuged at 1,000 g for 5 min to remove unbroken cells and cell debris and the resulting supernatant was used as the PNS fraction.

TIRF Microscopy

HEK293-Fc γ RII cells grown on poly-L-lysine coated 35mm glass bottom dish (1.5 \times 10⁵ cells/dish) were transfected with or without Stx2/3/4 siRNA. At 52 hr after transfection, cells were transfected with plasmid encoding GFP-DrrA₆₁₋₆₄₇, and incubated for an additional 20 hr. Transfected cells were permeabilized as described above. To prepare donor vesicles, HEK293-Fc γ RII cells were transfected with or without Sec22b siRNA. At 52 hr after transfection, cells were transfected with plasmid encoding RFP-KDEL for 20 hr and then cells were collected and disrupted in 700 μ l homogenization buffer as described above. The resulting PNS fraction (100 μ l) containing fluorescent vesicles was incubated with permeabilized cells in the presence of 0.5mM GTP for 90 min at room temperature. Cells were washed extensively and warmed to 37°C for 15 min on a temperature-controlled stage attached to the TIRF microscope. A field in which cells producing GFP-DrrA could be detected was selected for imaging. Time-lapse microscopy was initiated before the addition of 100 μ l of fusion buffer, which consisted of the PNS fraction from HEK293-Fc γ RII cells containing freshly added solutions of GTP and ATP to a final concentration of 0.5 mM. TIRF images were collected using an inverted microscope (IX-70; Olympus) fitted with a 60x NA 1.45 TIRFM lens (Olympus) and controlled by Andor iQ software (Andor Technology). Laser lines (488 and 568nm) from argon and argon/krypton lasers were coupled to the TIRFM condenser through a single optical fiber. The calculated evanescent field depth was ~100nm. Cells were imaged by excitation at 0.25Hz, without binning, with 0.5-s exposures and detected with a black illuminated electron-multiplying charge-coupled device camera (512x512 pixels; 16-bit; iXon887; Andor Technology). Image analysis was performed using ImageJ software (NIH).

Luciferase-KDEL recruitment and fusion assay

HEK293-Fc γ RII cells grown on poly-L-lysine-coated 24-well plates (1×10^5 cells/well) were permeabilized as describe above. Permeabilized cells were incubated with or without 3 μ g of purified His-DrrA for 1 hr at room temperature. Cells were washed and 100 μ l of a PNS fraction from HEK293-Fc γ RII cells was added either with or without GDP or GTP at 0.5 mM final concentration. Cells were incubated for 1 hr at room temperature and then washed extensively. To assay tethering, 100 μ l of lysis buffer (100mM NaCl, 1mM MgCl₂, 20mM Hepes-KOH (pH7.2), 1% Triton X-100 and protease inhibitors) was added to the cells to liberate Luciferase-KDEL from vesicles and activity was measured using a Luciferase assay kit (New England Biolabs). To measure vesicle fusion, in tethering reactions using Luciferase-KDEL vesicles and permeabilized cells conducted in parallel wells as described above. After the tethering reaction, 100 μ l of fusion buffer was added to the reaction, which consisted of PNS fraction from HEK293-Fc γ RII cells containing freshly added solutions of GTP and ATP to a final concentration of 0.5 mM. Luciferase-KDEL was collected in the reaction supernatant and samples were centrifuged at 100,000 g for 30 min to remove any intact vesicles. Luciferase-activity was measured in the cleared supernatant and compared to the Luciferase activity that remained associated with the permeabilized cells. Results were expressed as the ratio of Luciferase activity in the supernatant compared to Luciferase activity that remained cell-associated.

Ts045-VSVG-GFP recruitment and fusion assay

HEK293-Fc γ RII cells were transfected with a plasmid encoding ts045-VSVG-GFP (Presley et al., 1997) and incubated at the non-permissive temperature of 40° C. for 20 hr. To initiate exit of ts045-VSVG-GFP from the ER, cells were shifted to 32° C. for 15 min, 45 min, and 90 min and fixed. Cells were examined by fluorescence microscopy to determine the subcellular localization of ts045-VSVG-GFP. Vesicles containing ts045-VSVG-GFP were generated from cells shifted to the permissive temperature for either 15 min or 90 min using the protocol described for RFP-KDEL vesicles. Epifluorescence microscopy and TIRF microscopy studies to visualize the binding and fusion of ts045-VSVG-GFP to the PM of semi-intact cells was conducted as described above for RFP-KDEL-containing vesicles.

Supplementary Material

Refer to Web version on PubMed Central for supplementary material.

Acknowledgments

We wish to thank S. Shin, S. Mukherjee, S. Ivanov, and A. Hubber for their helpful discussions and assistance in manuscript preparation, M. Tagaya for experimental support, and B. Lindenbach for technical advice and for providing the plasmid encoding Luciferase-KDEL. This work was supported by NIH grants R01AI041699 (CRR) and DP2-OD002980-01 (DT).

References

- Ackerman AL, Giodini A, Cresswell P. A role for the endoplasmic reticulum protein retrotranslocation machinery during crosspresentation by dendritic cells. *Immunity*. 2006; 25:607–617. [PubMed: 17027300]
- Aoki T, Ichimura S, Itoh A, Kuramoto M, Shinkawa T, Isobe T, Tagaya M. Identification of the neuroblastoma-amplified gene product as a component of the syntaxin 18 complex implicated in Golgi-to-endoplasmic reticulum retrograde transport. *Mol Biol Cell*. 2009; 20:2639–2649. [PubMed: 19369418]
- Arasaki K, Roy CR. Legionella pneumophila promotes functional interactions between plasma membrane syntaxins and Sec22b. *Traffic*. 2010; 11:587–600. [PubMed: 20163564]

- Becker T, Volchuk A, Rothman JE. Differential use of endoplasmic reticulum membrane for phagocytosis in J774 macrophages. *Proc Natl Acad Sci U S A*. 2005; 102:4022–4026. [PubMed: 15753287]
- Berger KH, Isberg RR. Two distinct defects in intracellular growth complemented by a single genetic locus in *Legionella pneumophila*. *Mol Microbiol*. 1993; 7:7–19. [PubMed: 8382332]
- Brombacher E, Urwyler S, Ragaz C, Weber SS, Kami K, Overduin M, Hilbi H. Rab1 guanine nucleotide exchange factor SidM is a major phosphatidylinositol 4-phosphate-binding effector protein of *Legionella pneumophila*. *J Biol Chem*. 2009; 284:4846–4856. [PubMed: 19095644]
- Coers J, Kagan JC, Matthews M, Nagai H, Zuckman DM, Roy CR. Identification of Icm protein complexes that play distinct roles in the biogenesis of an organelle permissive for *Legionella pneumophila* intracellular growth. *Mol Microbiol*. 2000; 38:719–736. [PubMed: 11115108]
- Derre I, Isberg RR. *Legionella pneumophila* replication vacuole formation involves rapid recruitment of proteins of the early secretory system. *Infect Immun*. 2004; 72:3048–3053. [PubMed: 15102819]
- Dietrich LE, Boeddinghaus C, LaGrassa TJ, Ungermann C. Control of eukaryotic membrane fusion by N-terminal domains of SNARE proteins. *Biochim Biophys Acta*. 2003; 1641:111–119. [PubMed: 12914952]
- Ensminger AW, Isberg RR. *Legionella pneumophila* Dot/Icm translocated substrates: a sum of parts. *Curr Opin Microbiol*. 2009; 12:67–73. [PubMed: 19157961]
- Gagnon E, Duclos S, Rondeau C, Chevet E, Cameron PH, Steele-Mortimer O, Paiement J, Bergeron JJ, Desjardins M. Endoplasmic reticulum-mediated phagocytosis is a mechanism of entry into macrophages. *Cell*. 2002; 110:119–131. [PubMed: 12151002]
- Guermontprez P, Saveanu L, Kleijmeer M, Davoust J, Van Endert P, Amigorena S. ER-phagosome fusion defines an MHC class I cross-presentation compartment in dendritic cells. *Nature*. 2003; 425:397–402. [PubMed: 14508489]
- Hatsuzawa K, Tamura T, Hashimoto H, Hashimoto H, Yokoya S, Miura M, Nagaya H, Wada I. Involvement of syntaxin 18, an endoplasmic reticulum (ER)-localized SNARE protein, in ER-mediated phagocytosis. *Mol Biol Cell*. 2006; 17:3964–3977. [PubMed: 16790498]
- Horwitz MA. The Legionnaires' disease bacterium (*Legionella pneumophila*) inhibits phagosome lysosome fusion in human monocytes. *J Exp Med*. 1983; 158:2108–2126. [PubMed: 6644240]
- Houde M, Bertholet S, Gagnon E, Brunet S, Goyette G, Laplante A, Princiotta MF, Thibault P, Sacks D, Desjardins M. Phagosomes are competent organelles for antigen cross-presentation. *Nature*. 2003; 425:402–406. [PubMed: 14508490]
- Ingmundson A, Delprato A, Lambright DG, Roy CR. *Legionella pneumophila* proteins that regulate Rab1 membrane cycling. *Nature*. 2007; 450:365–369. [PubMed: 17952054]
- Jesch SA, Linstedt AD. The Golgi and endoplasmic reticulum remain independent during mitosis in HeLa cells. *Mol Biol Cell*. 1998; 9:623–635. [PubMed: 9487131]
- Kagan JC, Stein MP, Pypaert M, Roy CR. *Legionella* subvert the functions of Rab1 and Sec22b to create a replicative organelle. *J Exp Med*. 2004; 199:1201–1211. [PubMed: 15117975]
- Machner MP, Isberg RR. Targeting of host Rab GTPase function by the intravacuolar pathogen *Legionella pneumophila*. *Dev Cell*. 2006; 11:47–56. [PubMed: 16824952]
- Machner MP, Isberg RR. A bifunctional bacterial protein links GDI displacement to Rab1 activation. *Science*. 2007; 318:974–977. [PubMed: 17947549]
- McNew JA, Parlati F, Fukuda R, Johnston RJ, Paz K, Paumet F, Sollner TH, Rothman JE. Compartmental specificity of cellular membrane fusion encoded in SNARE proteins. *Nature*. 2000; 407:153–159. [PubMed: 11001046]
- Muller MP, Peters H, Blumer J, Blankenfeldt W, Goody RS, Itzen A. The *Legionella* effector protein DrrA AMPylates the membrane traffic regulator Rab1b. *Science*. 2010; 329:946–949. [PubMed: 20651120]
- Murata T, Delprato A, Ingmundson A, Toomre DK, Lambright DG, Roy CR. The *Legionella pneumophila* effector protein DrrA is a Rab1 guanine nucleotide-exchange factor. *Nat Cell Biol*. 2006; 8:971–977. [PubMed: 16906144]
- Nagai H, Kagan JC, Zhu X, Kahn RA, Roy CR. A bacterial guanine nucleotide exchange factor activates ARF on *Legionella* phagosomes. *Science*. 2002; 295:679–682. [PubMed: 11809974]

- Presley JF, Cole NB, Schroer TA, Hirschberg K, Zaal KJ, Lippincott-Schwartz J. ER-to-Golgi transport visualized in living cells. *Nature*. 1997; 389:81–85. [PubMed: 9288971]
- Rogers LD, Foster LJ. The dynamic phagosomal proteome and the contribution of the endoplasmic reticulum. *Proc Natl Acad Sci U S A*. 2007; 104:18520–18525. [PubMed: 18006660]
- Roy CR, Berger KH, Isberg RR. *Legionella pneumophila* DotA protein is required for early phagosome trafficking decisions that occur within minutes of bacterial uptake. *Mol Microbiol*. 1998; 28:663–674. [PubMed: 9632267]
- Schoebel S, Blankenfeldt W, Goody RS, Itzen A. High-affinity binding of phosphatidylinositol 4-phosphate by *Legionella pneumophila* DrrA. *EMBO Rep*. 2010; 11:598–604. [PubMed: 20616805]
- Schoebel S, Oesterlin LK, Blankenfeldt W, Goody RS, Itzen A. RabGDI displacement by DrrA from *Legionella* is a consequence of its guanine nucleotide exchange activity. *Mol Cell*. 2009; 36:1060–1072. [PubMed: 20064470]
- Segal G, Purcell M, Shuman HA. Host cell killing and bacterial conjugation require overlapping sets of genes within a 22-kb region of the *Legionella pneumophila* genome. *Proc Natl Acad Sci USA*. 1998; 95:1669–1674. [PubMed: 9465074]
- Suh HY, Lee DW, Lee KH, Ku B, Choi SJ, Woo JS, Kim YG, Oh BH. Structural insights into the dual nucleotide exchange and GDI displacement activity of SidM/DrrA. *Embo J*. 2009; 29:496–504. [PubMed: 19942850]
- Swanson MS, Isberg RR. Association of *Legionella pneumophila* with the macrophage endoplasmic reticulum. *Infect Immun*. 1995; 63:3609–3620. [PubMed: 7642298]
- Tilney LG, Harb OS, Connelly PS, Robinson CG, Roy CR. How the parasitic bacterium *Legionella pneumophila* modifies its phagosome and transforms it into rough ER: implications for conversion of plasma membrane to the ER membrane. *J Cell Sci*. 2001; 114:4637–4650. [PubMed: 11792828]
- Touret N, Paroutis P, Terebiznik M, Harrison RE, Trombetta S, Pypaert M, Chow A, Jiang A, Shaw J, Yip C, et al. Quantitative and dynamic assessment of the contribution of the ER to phagosome formation. *Cell*. 2005; 123:157–170. [PubMed: 16213220]
- Traub LM, Bannykh SI, Rodel JE, Aridor M, Balch WE, Kornfeld S. AP-2-containing clathrin coats assemble on mature lysosomes. *J Cell Biol*. 1996; 135:1801–1814. [PubMed: 8991092]
- Vogel JP, Andrews HL, Wong SK, Isberg RR. Conjugative transfer by the virulence system of *Legionella pneumophila*. *Science*. 1998; 279:873–876. [PubMed: 9452389]
- Zhu Y, Hu L, Zhou Y, Yao Q, Liu L, Shao F. Structural mechanism of host Rab1 activation by the bifunctional *Legionella* type IV effector SidM/DrrA. *Proc Natl Acad Sci U S A*. 2010; 107:4699–4704. [PubMed: 20176951]
- Zolov SN, Lupashin VV. Cog3p depletion blocks vesicle-mediated Golgi retrograde trafficking in HeLa cells. *J Cell Biol*. 2005; 168:747–759. [PubMed: 15728195]
- Zuckman DM, Hung JB, Roy CR. Pore-forming activity is not sufficient for *Legionella pneumophila* phagosome trafficking and intracellular growth. *Mol Microbiol*. 1999; 32:990–1001. [PubMed: 10361301]

Highlights

The *L. pneumophila* effector DrrA activates Rab1 and binds plasma membrane (PM) syntaxins

PM-localized Rab1 GTPase stimulates ER-derived vesicle tethering

SNARE protein Sec22b and PM-localized syntaxins promote ER-derived vesicle fusion

DrrA promotes remodeling of PM-derived organelles by ER-derived vesicles

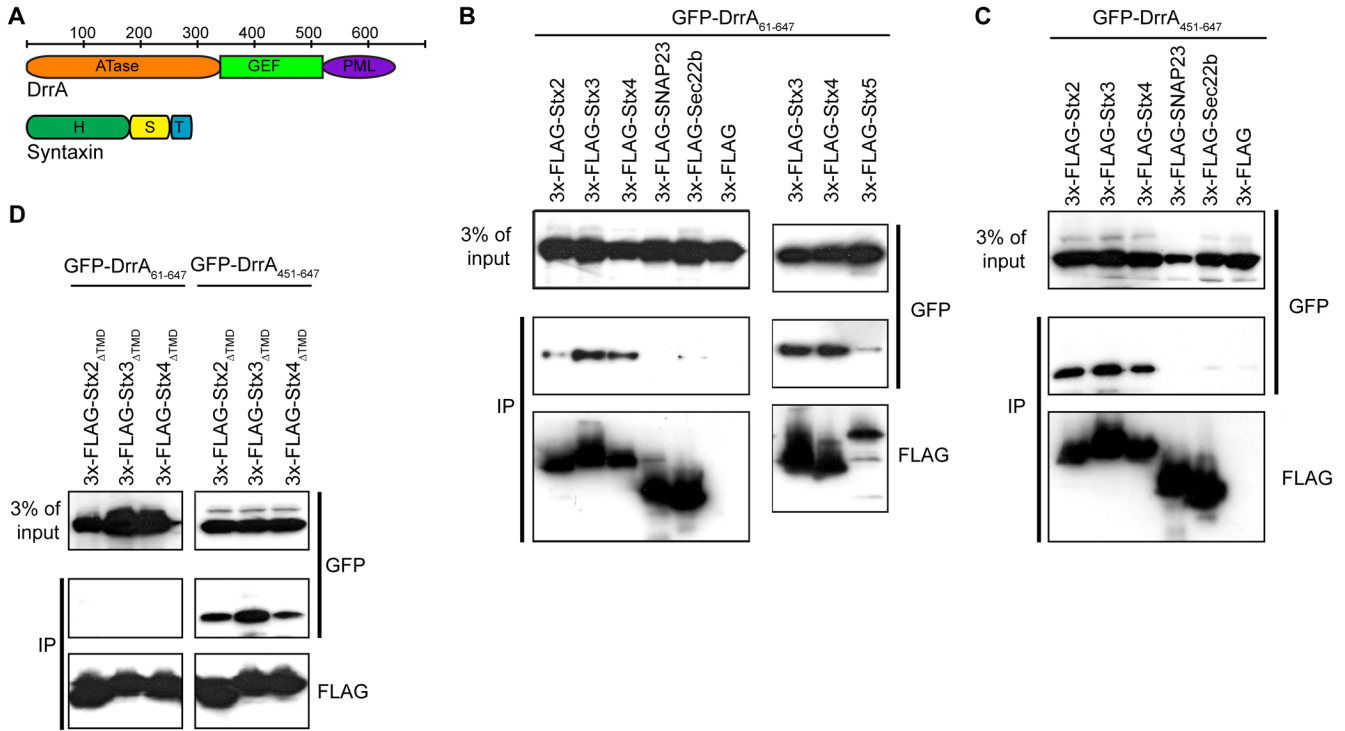


Figure 1. DrrA associates with PM syntaxins

GFP-tagged DrrA proteins and FLAG-tagged SNARE proteins were produced in HEK293-FcγRII cells and interactions were analyzed after the SNARE proteins from cells extracts were precipitated using anti-FLAG agarose. Immunoblot analysis using the antibodies indicated to the right of each blot show protein levels in the blots of the lysate (3% of input) and blots of the immunoprecipitate (IP). (A) Linear diagrams of the DrrA and syntaxin proteins with the bar on top indicating the position of amino acid residues that encompass structural domains in these proteins. The DrrA protein has an adenylyl transferase domain (ATase), a guanine nucleotide exchange factor domain (GEF) and a PM-localization domain containing a PI4P-binding region (PML). The syntaxin proteins have a Habc regulatory domain (H), a SNARE motif (S) and a transmembrane domain (TM). (B) The binding of GFP-DrrA₆₁₋₆₄₇ with the precipitated FLAG-tagged SNARE indicated on top of the panel was assessed by immunoblot analysis. (C) The binding of GFP-DrrA₄₅₁₋₆₄₇ with the precipitated FLAG-tagged SNARE indicated on top of the panel was assessed by immunoblot analysis. (D) The binding of GFP-DrrA₆₁₋₆₄₇ (left panels) and GFP-DrrA₄₅₁₋₆₄₇ (right panels) with the precipitated FLAG-tagged syntaxin proteins deleted of their transmembrane domain (ΔTMD) indicated on top of each panel was assessed by immunoblot analysis.

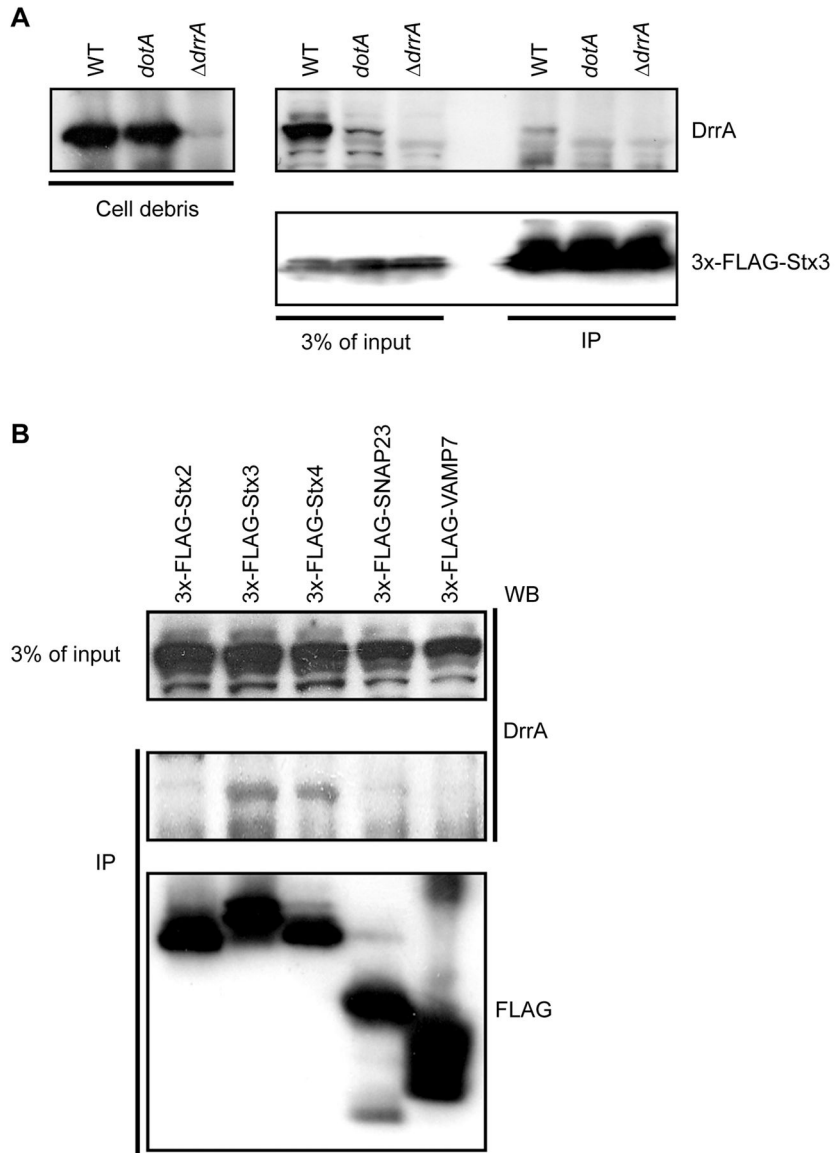


Figure 2. DrrA translocated into host cells during infection associates with PM syntaxins
 FLAG-tagged syntaxin proteins produced in HEK293-Fc γ R1I were infected with *Legionella* and precipitated using anti-FLAG agarose. Immunoblot analysis was used to determine the amount of DrrA translocated into cells during infection that coprecipitated with the FLAG-tagged syntaxins. (A) HEK293-Fc γ R1I cells producing 3x-FLAG-Stx3 were infected with wild type *Legionella* (WT), a Dot/Icm-deficient mutant (Δ *dotA*) or a mutant deficient in the DrrA protein (Δ *drrA*) as indicated above each lane. Intact intracellular bacteria were collected in the pellet after centrifugation of the cell lysate and the 3x-FLAG-Stx3 was precipitated from the cleared lysate using anti-FLAG agarose. Immunoblots show the amount of DrrA protein inside the intracellular bacteria (left panel). The top right anti-DrrA blot and the bottom right anti-FLAG blot show the amount of DrrA and 3xFLAG-Stx3 in the cleared host cell lysate (3% of input) and in the 3x-FLAG-Stx3 immunoprecipitate (IP), respectively. (B) HEK293-Fc γ R1I cells producing the indicated 3x-FLAG-tagged SNARE proteins were infected with wild type *Legionella* and proteins were precipitated from a lysate containing host cytosolic proteins using anti-FLAG agarose. The amount of

translocated DrrA in the cleared lysate (3% of input) and the amount of the 3x-FLAG-tagged protein and DrrA protein in the immunoprecipitate (IP) was determined by immunoblot analysis.

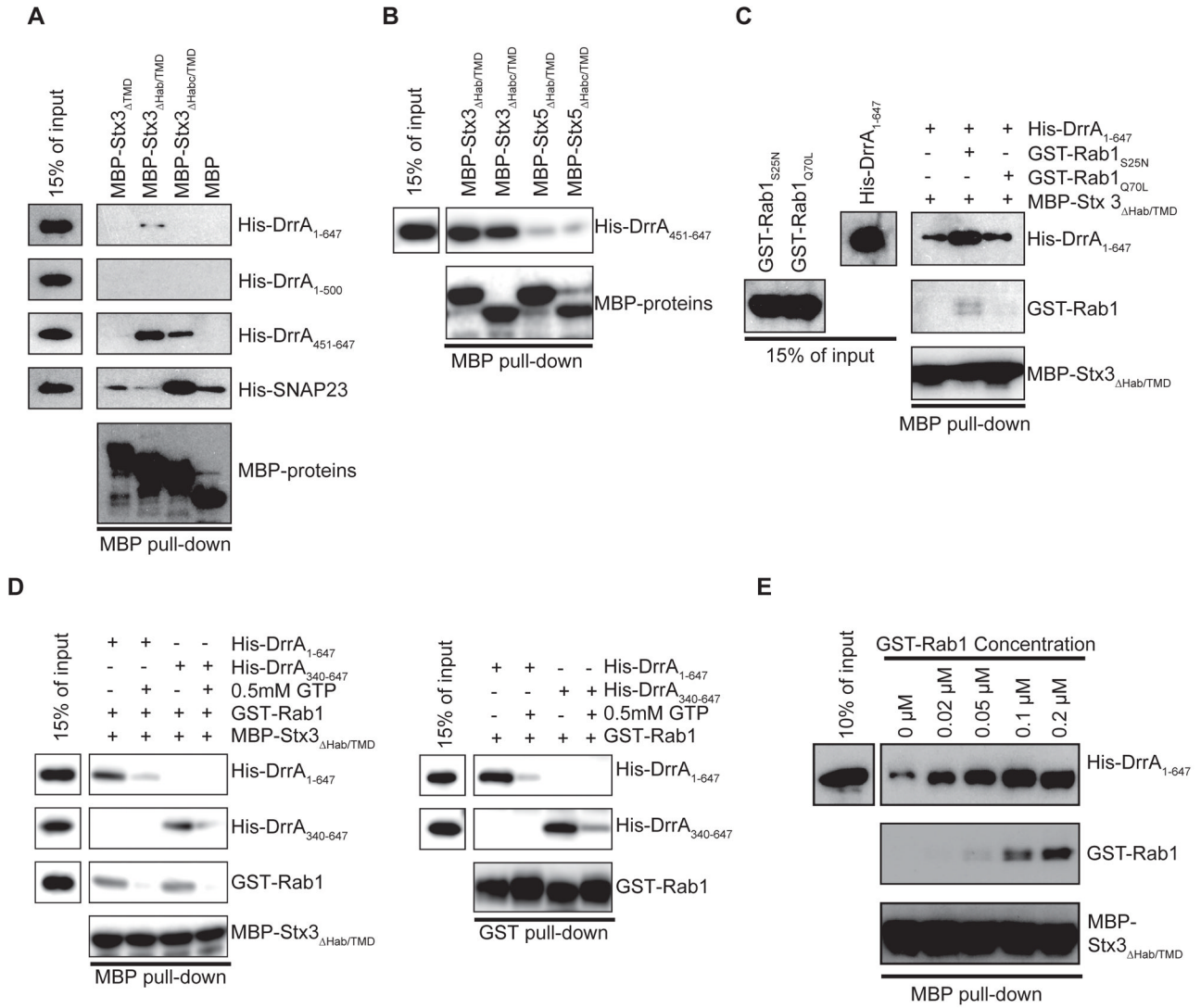


Figure 3. Rab1 regulates DrrA binding to the SNARE motif in Stx3

In vitro interactions between MBP-tagged syntaxin proteins and purified DrrA proteins were assayed using amylose agarose to pull down MBP protein complexes. Proteins in the reaction (15% of input) and in the MBP pull-down were separated by SDS-PAGE and detected using antibodies specific for either the His, GST or MBP tag as indicated on the right of each blot. (A) Purified Stx3 derivatives fused to MBP indicated on the top were incubated with purified His-tagged DrrA proteins indicated on the right. MBP alone was included as a control for non-specific interactions. His-SNAP23 was included as a positive control for functional SNARE interactions with Stx3. (B) Purified Stx3 and Stx5 proteins fused to MBP are indicated on the top were incubated with His-DrrA₄₅₁₋₆₄₇. (C) Purified His-DrrA₁₋₆₄₇, GST-Rab1_{S25N} or GST-Rab1_{Q70L} derivatives, and MBP-Stx3_{ΔHab/TMD} were included in the *in vitro* reaction as indicated in the grid on top of the panel. (D) Purified His-DrrA₁₋₆₄₇, His-DrrA₃₄₀₋₆₄₇, GST-Rab1, and MBP-Stx3_{ΔHab/TMD} were incubated either in the presence or absence of 0.5mM GTP *in vitro* as indicated in the grid on top of each panel. The MBP pull-down panel (left) shows proteins bound to the MBP-tagged fusions isolated on amylose beads. The GST pull-down panel (right) shows proteins bound to GST-tagged Rab1 isolated on glutathione beads. This control shows that DrrA₁₋₆₃₇

and DrrA₃₄₀₋₆₄₇ bound similarly to GST-Rab1 and that complex formation was less efficient in the presence of GTP. (E) Purified His-DrrA₁₋₆₄₇ and MBP-Stx3 $\Delta_{Hab/TMD}$ were added to each reaction at an equal molar ratio (0.1 μ M) and incubated with the indicated concentrations of purified GST-Rab1.

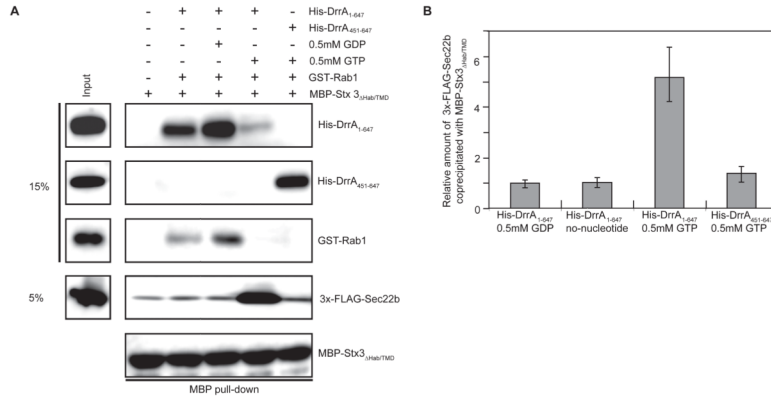


Figure 4. DrrA and Rab1 coordinate Stx3 interactions with Sec22b
 The binding of purified MBP-Stx3 $\Delta_{Hab/TMD}$ to vesicle-associated 3x-FLAG-Sec22b was assayed using amylose agarose to pull down MBP protein complexes. (A) Purified MBP-Stx3 $\Delta_{Hab/TMD}$ was incubated *in vitro* with the purified His-DrrA derivatives, GST-Rab1 and nucleotides indicated in the grid above each lane. A PNS fraction containing vesicles displaying 3x-FLAG-Sec22b was incubated with each reaction. Proteins in the reaction (15% or 5% of input) and in the MBP pull-down were separated by SDS-PAGE and detected using antibodies specific for either the His, GST, FLAG or MBP tag as indicated on the right of each blot. (B) Blots from the experiment shown in panel A were scanned to determine relative amounts of 3xFLAG-Sec22b associated with MBP-Stx3 $\Delta_{Hab/TMD}$. Relative amounts of 3x-FLAG-Sec22b were calculated by dividing the signal intensity observed for reaction conditions indicated below each bar by the signal intensity in the control lane where MBP-Stx3 $\Delta_{Hab/TMD}$ alone was used to pull-down 3x-FLAG-Sec22b on vesicles. Data represent the mean \pm SEM of four independent experiments.

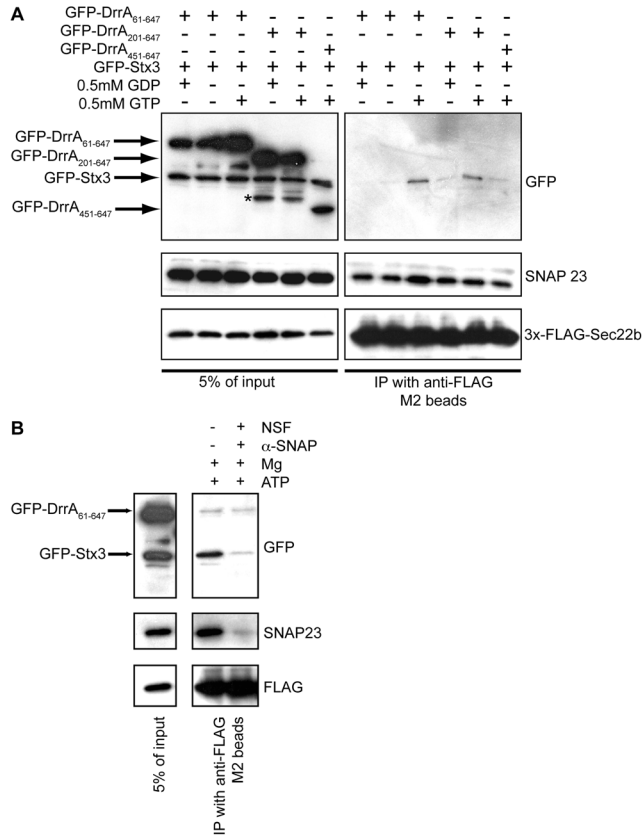


Figure 5. DrrA coordinates the functional pairing of Stx3 and Sec22b in permeabilized cells
 Permeabilized HEK293-FcγRII cells producing the indicated GFP-Stx3 and GFP-DrrA proteins were incubated with vesicles displaying 3x-FLAG-Sec22b and protein complexes were precipitated using anti-FLAG agarose. (A) The GFP-DrrA and 3x-FLAG-Stx3 constructs expressed in the permeabilized HEK293-FcγRII cells and the inclusion of GTP or GDP in the reactions are indicated above each lane. Immunoblot analysis using antibodies specific for GFP, SNAP23, and FLAG show protein levels in the reaction (5% or input, left panels) and protein levels in the anti-FLAG immunoprecipitate (IP, right panels). Because SNAP23 has been shown to form a SNARE complex with Sec22b and Sec18, this interaction served as a positive control. (B) As in panel A, HEK293-FcγRII cells producing GFP-Stx3 and GFP-DrrA₆₁₋₆₄₇ were permeabilized and incubated with vesicles in a PNS fraction obtained from cells producing 3x-FLAG-Sec22b in the presence of GTP. Lysates of these reactions were incubated in the presence or absence of purified NSF and α-SNAP as indicated. Protein levels in the reaction (5% or input) and protein levels in the 3x-FLAG-Sec22b immunoprecipitate (IP) were determined by immunoblot analysis using antibodies specific for GFP, SNAP23, and FLAG.

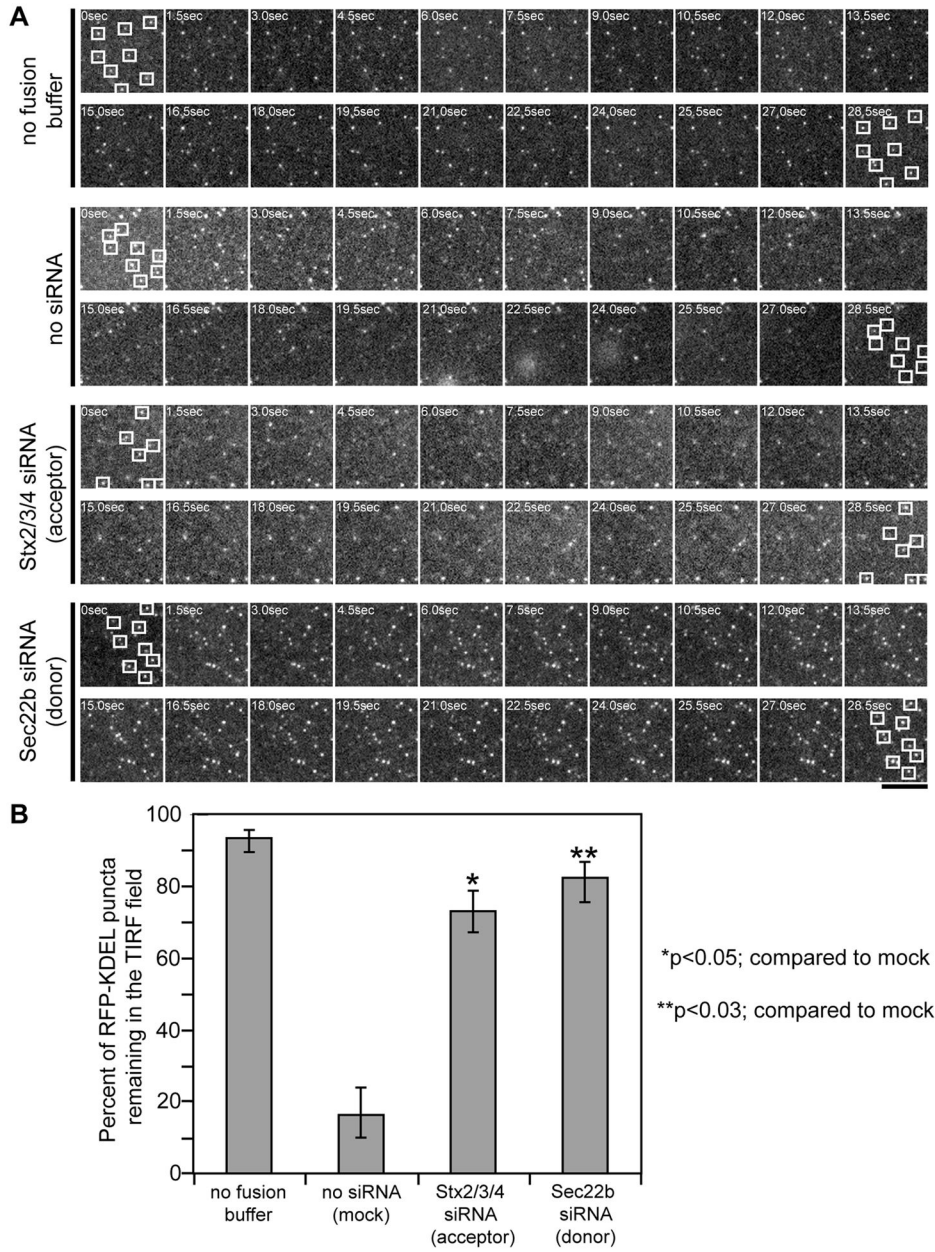


Figure 6. DrrA alters ER-derived vesicle dynamics at the PM

Cells producing GFP-DrrA₆₁₋₆₄₇ were permeabilized and incubated with ER-derived vesicles containing RFP-KDEL. TIRF microscopy was used to image ER-derived vesicles associated with the PM in cells producing GFP-DrrA₆₁₋₆₄₇. (A) A series of time-lapse micrographs showing vesicle dynamics without the addition of fusion buffer was included to demonstrate the stability of vesicle tethering. Upon the addition of fusion buffer vesicle dynamics were imaged in cells that had not been treated with siRNA (no siRNA), in cells where siRNA was used to reduce the levels of the proteins Stx2, Stx3, and Stx4 in the permeabilized cells (acceptor), and in cells where siRNA was used to reduce the levels of Sec22b in the in the (donor) cells producing RFP-KDEL. Squares show the location of randomly chosen vesicles at the beginning and end of each series. Bar, 1µm. (B) Time-lapse video TIRF microscopy images captured as described in panel A were used to follow RFP-

KDEL-positive vesicles tethered in the TIRF plane. Vesicles (RFP-KDEL puncta) that were tethered in the TIRF plane upon the addition of fusion buffer (t=0 sec) were followed over time (30 sec). Data show the percent of vesicles present in the TIRF plane at t=0 sec that remained in the TIRF plane at t=30 sec, and represents the mean \pm SEM of three independent experiments in which 100 vesicles were scored for each series. $p^* < 0.05$, $p^{**} < 0.03$ compared to the no siRNA (mock) control.

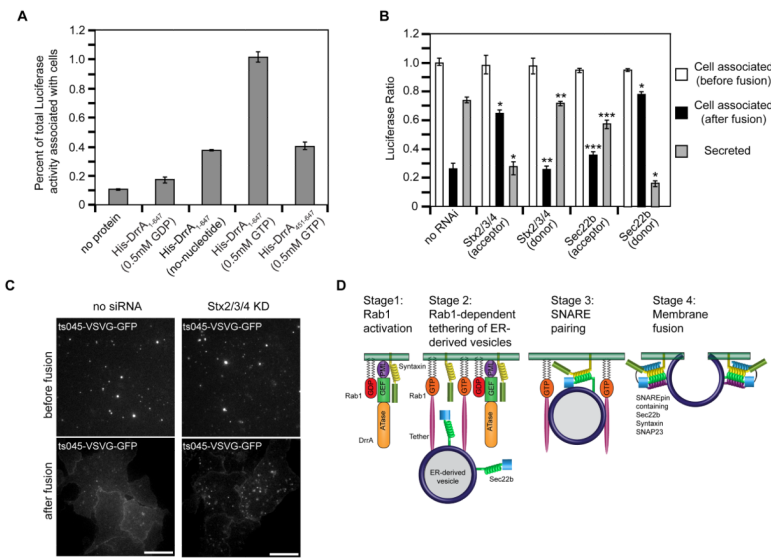


Figure 7. SNARE programming by DrrA and Rab1 promotes fusion of ER-derived vesicles with the PM

Tethering and fusion of ER-derived vesicles containing Luciferase-KDEL or ts045-VSVG-GFP with the PM of permeabilized HEK293-FcγRII cells was measured *in vitro*. (A) Permeabilized HEK293-FcγRII cells were incubated with purified His-DrrA protein either in the presence or absence of nucleotides as indicated. After the addition of a PNS fraction from cells producing Luciferase-KDEL, the tethering of ER-derived vesicles was assessed by determining the Luciferase activity associated with the permeabilized cells, which is presented as the percent of total Luciferase activity added to the reaction. (B) Permeabilized HEK293-FcγRII cells were incubated with purified His-DrrA₁₋₆₄₇ protein and a PNS fraction from cells producing Luciferase-KDEL was added. Tethering and fusion of ER-derived vesicles was assessed independently in parallel wells. The tethering of ER-derived vesicles was assessed by determining the Luciferase activity associated with the permeabilized cells, which is presented as the percent of total Luciferase activity added to the reaction (white bars, cell associated before fusion). Fusion was assessed by comparing the Luciferase activity that remained cell associated after the addition of fusion buffer (black bars) to the Luciferase activity that was liberated into the supernatant (gray bars, secreted). Shown are reactions in which siRNA was used to reduce the levels of the proteins Stx2, Stx3, and Stx4 (Stx2/3/4) or Sec22b in the permeabilized cells (acceptor), and reactions in which siRNA was used to reduce the levels of the proteins Stx2, Stx3, and Stx4 (Stx2/3/4) or Sec22b in the (donor) cells producing Luciferase-KDEL. These data are presented as a ratio of the total Luciferase activity that was associated with cells before fusion. Data are the means ± SEM of three independent experiments. *p<0.05 when compared to the same fraction in no RNAi samples; **p<0.01 when compared to the same fraction in Stx2/3/4 (acceptor) samples; ***p<0.01; compared to the same fraction in Sec22b (donor) samples. (C) Vesicles prepared from cells 15 min after ts045-VSVG-GFP was released from the ER were added to permeabilized control cells (no siRNA) or permeabilized cells in which PM syntaxins had been silenced (Stx2/3/4 KD). TIRF images show tethered ts045-VSVG-GFP-positive vesicles at the PM (before fusion) and the change in ts045-VSVG-GFP fluorescence that occurred after the addition of fusion buffer (after fusion). (D) A model that depicts data on how DrrA could promote the tethering and fusion of ER-derived vesicles with a PM-derived organelle. The first stage shows DrrA recruiting Rab1-GDP to the membrane and associating with Stx3. In the second stage the GEF activity of DrrA activates Rab1 on the PM-derived organelle, and active Rab1 is required for the association of ER-derived vesicles

displaying Sec22b. A tethering factor that binds to active Rab1 is predicted to be involved. In the third stage Sec22b and Stx3 interactions result from vesicle tethering. In the final stage the fusion of ER-derived vesicles with the PM-derived organelle membrane is mediated by the assembly of a functional SNARE complex (SNAREpin) consisting of the v-SNARE Sec22b and the t-SNARE comprised of Stx3 and SNAP23.